

Accepted Manuscript

Preparation and characterization of PVA/GA/Laponite membranes to enhance pervaporation desalination performance

Asmaa Selim, Andras Jozsef Toth, Eniko Haaz, Daniel Fozzer, Agnes Szanyi, Nora Hegyesi, Peter Mizsey

PII: S1383-5866(19)30811-1
DOI: <https://doi.org/10.1016/j.seppur.2019.03.084>
Reference: SEPPUR 15451

To appear in: *Separation and Purification Technology*

Received Date: 28 February 2019
Revised Date: 27 March 2019
Accepted Date: 27 March 2019

Please cite this article as: A. Selim, A. Jozsef Toth, E. Haaz, D. Fozzer, A. Szanyi, N. Hegyesi, P. Mizsey, Preparation and characterization of PVA/GA/Laponite membranes to enhance pervaporation desalination performance, *Separation and Purification Technology* (2019), doi: <https://doi.org/10.1016/j.seppur.2019.03.084>

This is a PDF file of an unedited manuscript that has been accepted for publication. As a service to our customers we are providing this early version of the manuscript. The manuscript will undergo copyediting, typesetting, and review of the resulting proof before it is published in its final form. Please note that during the production process errors may be discovered which could affect the content, and all legal disclaimers that apply to the journal pertain.



Preparation and characterization of PVA/GA/Laponite membranes to enhance pervaporation desalination performance

Asmaa Selim^a, Andras Jozsef Toth^a, Eniko Haaz^a, Daniel Fozer^a, Agnes Szanyi^a, Nora Hegyesi^d, Peter Mizsey^{a,b}

^a Department of Chemical and Environmental Process Engineering, Budapest University of Technology and Economics, 1111 Budapest, Hungary.

^b Department of Fine Chemicals and Environmental Technologies, University of Miskolc, 3515 Miskolc, Hungary.

^d Laboratory of Plastics and Rubber Technology, Department of Physical Chemistry and Materials Science, Budapest University of Technology and Economics, Budapest, Hungary.

Abstract

Pervaporation (PV) has shown great promise in water desalination technology. In this work, laponite XLG - Poly (vinyl alcohol) (PVA-Lap) mixed matrix membranes (MMMs) were fabricated to investigate the elaboration of desalination of high-salinity water by pervaporation. The influence of laponite content on the morphology, chemical structure and hydrophilicity of the membranes was investigated. In addition, salt transport properties in the membranes were observed. Moreover, the effect of different laponite content in the PVA matrix on the desalination performance was observed at temperatures from 40°C to 70 °C and feed solutions with up to 10 wt% NaCl. The prepared MMMs showed higher hydrophilicity and roughness of the surface and higher mechanical stability. The higher water flux of 58.6 kg/m².h with a salt rejection over 99.9 % was achieved using 2 wt% laponite XLG MMMs desalinating 3 wt% aqueous NaCl solution at 70 °C. The salt permeability in the membrane was lower by two orders of magnitude than that of water. The water/salt selectivity increased, while the water permeability decreased, with increasing of laponite content in the membrane.

Keywords

Pervaporation, Desalination, Salt transport, Poly (vinyl alcohol), Laponite, Mixed matrix membranes.

1. Introduction

Fresh water scarcity has materialized a serious threat to human livings and social developments. Due to the spectacular increase in the population and water pollution, it is necessary to find engineering solutions to provide fresh water in many water-limited areas [1, 2]. One of the most effective methods to produce fresh water from salt water such as brackish water and seawater is the desalination technology [3]. Nowadays, membrane technology is considered as an attractive desalination way, counting on of their high efficiency, potential energy savings, high operational stability, low chemical costs, ease of integration and scale-up compared with traditional distillation techniques [4, 5].

In recent years, membrane distillation (MD) and pervaporation (PV) have become an appealing alternative for dealing with high-saline water and having the ability to resist certain type of fouling. Although MD shows a promising way for high-salinity water desalination, membrane fouling and wetting are recognized as challenging problems leading to crucial disadvantage and result in increasing the costs of the process essentially for operating over long-term [6]. Alternatively, PV is another membrane process which has been reported as a prospective process for desalination due to its potential in energy efficiency and feasibility in handling high salinity water [7-9].

Pervaporation (PV) has primarily reported for liquid separation, such as dehydration process for the water from the serviceable organic solvents using hydrophilic membranes, or using hydrophilic membranes to remove the traces of several organic solvent from an aqueous solution. On the other hand, the specific organoselective membranes have been used for organic-organic mixtures separation [10-12]. The mass transport process in PV is based on the widely-accepted solution-diffusion model. Typically, a preheated liquid mixture is directly contacted with the feed side of a PV membrane and leaves the membrane in a gaseous state which is then condensed by a cold medium on permeate side which is maintained by vacuum [13]. According to the solution-diffusion model for PV desalination, the adsorbed

water molecules on the surface of the hydrophilic membrane are posteriorly diffuse through the membrane and eventually converted to vapor on the permeate side. Therefore, owing to the non-volatility of salt in the feed, using pervaporation membrane can achieve high salt rejection as well as the rejection of volatile organics granting highly pure water production [14].

Hydrophilic dense polymeric membranes with high solubility of water are considered the most ideal for the pervaporation desalination process such as cellulose [15], polyether amide [8], poly(ether-block-amide) (PEBA) [16], and poly(vinyl alcohol) [9, 17, 18]. Despite these membranes have achieved high ion rejection, the reported water flux was commonly low and still needs to be improved for PV desalination. Moreover, the instability and the low mechanical strength in hot water due to the high hydrophilicity, inhibit the potential application of PV in desalination. Recently, mixed matrix membranes have attracted great interest for pervaporation process due to their remarkable advantages of both polymer and inorganic materials. After recognizing these combined advantages, different researchers developed MMMs for pervaporation desalination such as PVA/silica [14], GO/CS [19], and PVA/PVDF/GO [20].

Poly(vinyl alcohol) (PVA) has been widely used for pervaporation process owing to its high hydrophilicity, film-forming ability, resistance to organic pollution, non-toxicity, biodegradable and chemical/thermal stability. PVA is a water –soluble synthesis polymer with -OH groups on its backbone, which crucially provides distinguishing sorption and diffusion of water in it and facilitate its modification [21-23].

Recently, PVA-nanoclays are well-established components for pervaporation separation process. The commonly used nanoclays are clinoptilolite, montmorillonite, and Bentonite [24-26]. Laponite is a synthetic nanoclay consisting of a layered structure with 30 nm diameter and 1 nm in thickness with empirical formula $\text{Na}^{+0.7}[(\text{Mg}_{5.5}\text{Li}_{0.3})\text{Si}_8\text{O}_{20}(\text{OH})_4]^{-0.7}$ and considered as belonging to smectic clay family. Laponite clay has significant properties such as high biocompatibility, anisotropic and great surface area along with its great ability for cationic exchange. Although, laponite clay is a well-established component for drug delivery, tissue engineering and wound healing applications [27-29]. Additionally, Laponite clay is

highly hydrophilic and exfoliates easily in water and has been widely used in the synthesis of mechanically strong nanocomposite polymers as also has the ability to enhance the physical properties of hydrogels [30-33]. However, to the best of the author's knowledge, no researchers has studied so far the effect of laponite clay on pervaporation performance.

This paper reports about a new MMMs of laponite XLG clay / PVA for desalination by pervaporation. The MMMs were synthesized via exfoliation of the nanoclay in the polymer solution with Glutaraldehyde (GA) as crosslinker agent followed by casting procedure. The effect of laponite incorporation on the chemical structure, surface morphology, hydrophilicity, and mechanical properties of the MMMs was studied by, Fourier transform infrared spectroscopy (FTIR), scanning electron microscope (SEM), sessile drop contact angle assessment and tensile apparatus, respectively. The pervaporation desalination performance of laponite/PVA membranes was studied varying concentration of NaCl aqueous in respect to permeate flux as also salt rejection. The transport properties of NaCl and water through the membranes such as partition, diffusion and permeability coefficients were discerned and evaluated for recognizing the mechanism of the salt transport and separation of PV desalination process.

2. Experimental

2.1. Materials

Poly(vinyl alcohol) $(C_2H_4O)_x$ with MW of 85000-124000 g/mol and 99%+ hydrolyzed; Glutaraldehyde (GA) $(C_5H_8O_2)$ grade II with 25% in water were purchased from Sigma-Aldrich Chemie GmbH. (Schnelldorf, Germany). Sodium chloride (NaCl) was obtained from Reanal Chemicals Ltd. (Budapest, Hungary). Laponite XLG ($\rho = 2.53 \text{ g/cm}^3$, CEC = 0.55 meq/g, $d = 25\text{--}30 \text{ nm}$, $h = 0.92 \text{ nm}$) was supplied by Laboratory of Plastics and Rubber Technology, Department of Physical Chemistry and Materials Science, Budapest University of Technology and Economics, and was purchased from Byk Additives and Instruments. All chemicals were used as such without further purification.

2.2. Fabrication of MMMs

Certain amount of PVA powder was dissolved in deionized water under robust stirring at 90 °C to obtain a homogeneous clear solution. In separate flask certain mass of Laponite XLG was dispersed in 10 ml of deionized water by sonication for 3 h to get a clear solution, indicating good dispersion of the nanofiller. The PVA solution was mixed with the above suspension to obtain 5% PVA casting solution with different concentration of Laponite XLG (0, 2 wt%, 5 wt%, 7 wt%, and 10 wt% of Laponite with respect to the dry polymer weight). After being stirred for 24 h in situ cross-linking was done by adding a certain amount of glutaraldehyde and the solution pH was adjusted with 37% HCl solution and the system was vigorously stirred for 3-5 min. Then final solutions were cast onto Petri dishes and totally dried at room temperature. After annealing for 3 h in an oven at 40°C the PVA membrane and the PVA-Laponite membranes were picked up and were designed as PVA, PVA-Lap2, PVA-Lap5, PVA-Lap7, and PVA-Lap10 corresponding to the Laponite XLG content as mentioned above. The thickness of pristine PVA and PVA/Laponite mixed matrix membranes was measured at different points across the membrane using a thickness gauge and confirmed by SEM measurements in the range of 120-160 μm . A simple scheme showing the steps used for preparing PVA-Laponite XLG MMMs can be seen in Figure 1.

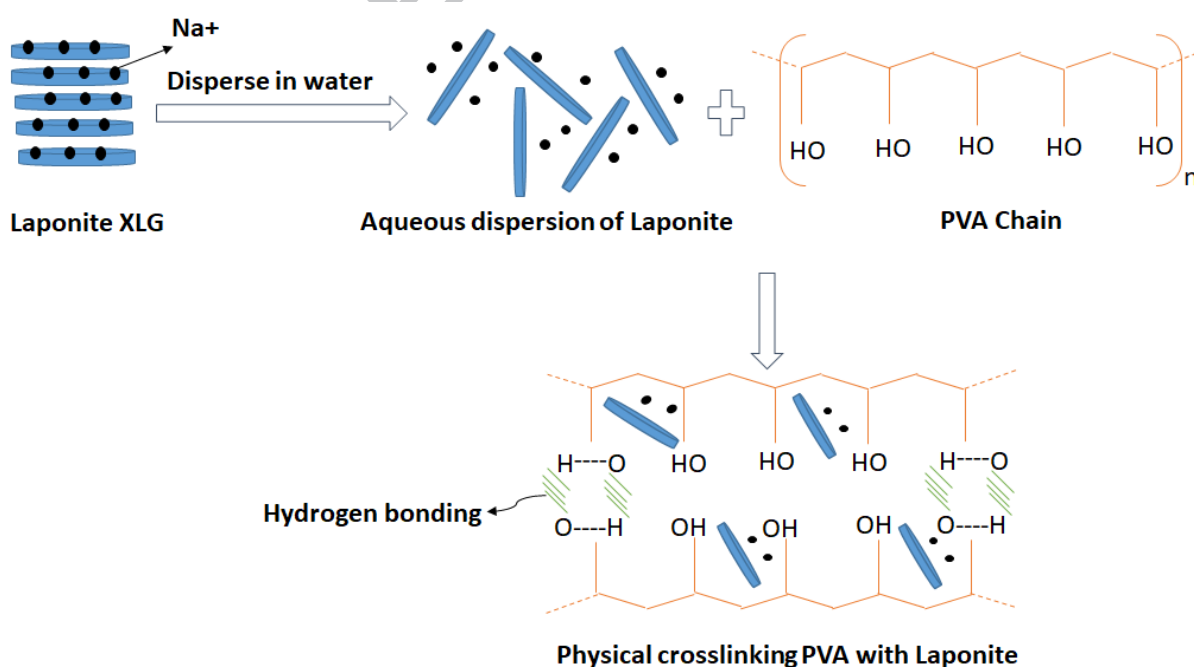


Figure 1: Simple Scheme for the fabrication of PVA-Laponite MMMs.

2.3. Characterization of Laponite powder and PVA-Laponite MMMs

Morphology and chemical structure

The crystallinity of Laponite XLG and MMMs membranes was investigated by X-ray diffraction (PANalytical X'Pert Pro MPD X-ray diffractometer at room temperature) with 2θ from 5° to 65° .

The surface morphology of Laponite powder, PVA plain membrane, and laponite –loaded MMMs was studied using Scanning electron microscope (SEM, JEOL JSM-5500LV) after covering the sample with gold.

A Fourier transform infrared spectroscopy (ATR mode of FTIR, BRUKER Tensor-37) was utilized to analyse the chemical linking of the powder laponite, PVA membrane and MMMs in the range of $500\text{--}4000\text{ cm}^{-1}$.

Thermal properties and degradation temperatures of Laponite powder, PVA plain membrane, and laponite–loaded MMMs were operated by thermogravimetric analysis (Perkin Elmer TGA-6) at temperature ranging from 35°C to 700°C at a heating rate of $10^\circ\text{C}/\text{min}^{-1}$. Each sample had of $5\text{--}10\text{ mg}$. After loading the samples into alumina pan they were heated under nitrogen atmosphere. Recording was done of temperature, sample weight, and differential weight. Differential weight is useful in derivative thermogravimetric analysis (DTG).

Hydrophilicity

Laponite addition effects on the PVA membrane surface hydrophilicity was investigated. This was done using a contact angle meter (KRÜSS, DSA 30, Germany) which provided water contact angle. In each film surface five locations were measured at room temperature and their average was used.

The membrane water uptake was calculated as the difference in weight between the weight of swollen membrane and that of dry membrane. For this, the dry membrane weight was taken and immersion in DI water was done for 24 h at room temperature. The membrane which was swollen removed from the water wiped gently and thoroughly using a filter paper when the water on the membrane surface gets completely removed and then it was weighted. For calculation of the water uptake of the membrane the following equation was used

$$\text{Water uptake} = \frac{W_{\text{swollen}} - W_{\text{dry}}}{W_{\text{dry}}} \times 100\% \quad (1)$$

Where, W_{swollen} (g) and W_{dry} (g) are the weight of swollen and dry membrane, respectively. Each membrane was measured three times and the average was taken as the final result.

Mechanical properties

An universal testing apparatus (INSTRON-5566) was used to evaluate the mechanical properties of the shaped membrane with a dimension of 60 mm × 10 mm and at 10 mm/min of speed. Each membrane was evaluated five times and the average value was taken.

2.4. Pervaporation experiment

The pervaporation desalination performance of the PVA and PVA-Lap MMMs was studied using a lab-scale P-28 membrane unit from CM-Celfa Membranetechnik AG vacuum Pervaporation apparatus as published in our previous paper [13]. The membrane under test was kept on a sintered disc in the membrane cell. The effective area of the membrane is 28 cm². For the test, the concentration of the feed solution was changed from 0 to 10 wt.% NaCl aqueous solutions. After adjusting the temperature in a range of 40–70 °C, the feed solution was subjected to circulation at flow rate of ~182 L/h through the cell. Low pressure of 6 torr was kept at permeate side and for this a vacuum pump was used which maintained the required vapor pressure difference across the membrane. The permeate was collected in cold traps refrigerated by liquid nitrogen at hourly basis. Water flux and salt rejection were adopted to investigate membrane desalination performance. The flux, J (kg/m².h) depended on the weight, W (Kg) of permeate in the cold trap, the membrane effective area, A (m²) and the time, t (h). It is calculated using the following equation:

$$J = \frac{W}{A \times t} \quad (2)$$

The salt rejection (R) was determined from the concentration of the feed (C_f) and the permeate (C_p) which were calculated from the measured conductivity using an electrical conductivity meter (Mettler Toledo FiveEasy) using the following equation:

$$R = \frac{C_f - C_p}{C_f} \times 100\% \quad (3)$$

2.5. Salt transport properties

Salt transport properties play Pivotal functions for evaluating the performance of desalination membrane. Salt transport properties of crosslinked PVA and PVA-Laponite MMMs were determined using a kinetic desorption technique in terms of NaCl diffusivity, D_s [34, 35]. First, the membrane with a known thickness was immersed in 50 ml of 5 wt% NaCl aqueous solution at room temperature for 48 h to make sure that the membrane is in equilibrium of NaCl and then removed followed by wiping off. Then the membrane was quickly placed in a beaker with 50 mL of DI water and continuously stirred at 600 rpm. The conductivity of the solution was monitored using a conductivity meter and recorded at 5 sec interval at room temperature and using standard curve of NaCl concentration with conductivity the values were converted to NaCl concentration. Desorption experiment results were correlated to the Fickian diffusion model by which the diffusivity D_s (cm^2/s) of NaCl in the membrane was obtained by plotting (M_t/M_∞) vs $t^{1/2}$ [34-36]

$$D_s = \frac{\pi \times l^2}{16} \left[\frac{d(M_t/M_\infty)}{d(t^{1/2})} \right]^2 \quad (4)$$

Where, l is the average membrane thickness, M_t is NaCl amount in the solution at t moment during desorption and M_∞ is the total mass of NaCl desorbed during the desorption experiment.

2.5.1. Salt solubility of membrane

The salt (NaCl) solubility, also named as sorption or partition coefficient (K_s), is defined as the ratio of the volumetric concentration of NaCl in the membrane to the original solution concentration (i.e. 5 wt %) which can be described as follows [37, 38]:

$$K_s = \frac{g \text{ NaCl}(M_\infty)/\text{cm}^3 \text{ membrane}}{g \text{ NaCl}/\text{cm}^3 \text{ solution}} \quad (5)$$

2.5.2. Salt permeability of membrane

According to the solution-diffusion model, NaCl permeability, P_s (cm^2/s) is defined as the product of D_s and K_s [39, 40]:

$$P_s = D_s \times K_s \quad (6)$$

2.6. Water/salt permeation selectivity of membrane

The membrane selectivity can be defined as the ratio of water permeability coefficient (P_w) to that of salt (P_s) and it can be adopted for membrane evaluation for inherent capability of membrane for water/salt separation and this could be express using the equation [37] :

$$\alpha_{w/s} = \frac{P_w}{P_s} \quad (7)$$

2.6.1. Water permeability of membrane

The solution-diffusion mechanism can be used to describe water transport in PV desalination membranes. According to the model when applying suitable vacuum in the permeate side, the water flux can be consistent with the concentration in the feed side (C_{wf} , g/cm^3), permeability (P_w , cm^2/s) of the specific component, and the thickness of the membrane (δ , cm) in theory [41, 42]:

$$J_i = \frac{D_i K_i}{\delta} C_{if} \quad (8)$$

From Eq. (7 and 8), The water permeability coefficient, P_w can be obtained from PV desalination water flux with pure water as feed as follows [4, 42] :

$$P_w = \frac{J_w \delta}{c_{wf}} \quad (9)$$

3. Results and discussion

3.1. Characterization of Laponite powder and PVA-Laponite MMMs.

Morphology and chemical structure

The XRD patterns in Fig.2 show the degree of crystallinity of the Laponite XLG powder, neat PVA membrane, and PVA-Laponite MMMs. For the pristine PVA membrane, a sharp diffraction peak around $2\theta = 19.5^\circ$ can be observed which represents the typical crystalline phase of PVA chain [43]. The XRD profile of powder laponite XLG manifests a broad pattern designate the low crystallinity and the small particle size. Sharp peaks are present at values of 19.8° , 35.3° , and 60.8° corresponding to (100), (110), and (300) crystal planes, respectively and a wide broad peak at 27.5° represent the (005) plane and these were reported also in previous papers [28, 31]. By comparison, the pattern of PVA-Lap2 MMMs shows absence of clear diffraction peaks between $2\theta = 20 - 65^\circ$. The sharp peak at 19.5° was also significantly weakened after exfoliation of laponite clay. This demonstrates that the exfoliated laponite XLG platelets are individually well dispersed in the PVA matrix and the polymer matrix is completely interpolated with it forming a compatible nanocomposite [44-46]. However, increasing the laponite content to 10% in PVA-Lap10 led to a narrow peak at $2\theta = 31.8^\circ$ which could indicate the possibility of intercalation or phase separation.

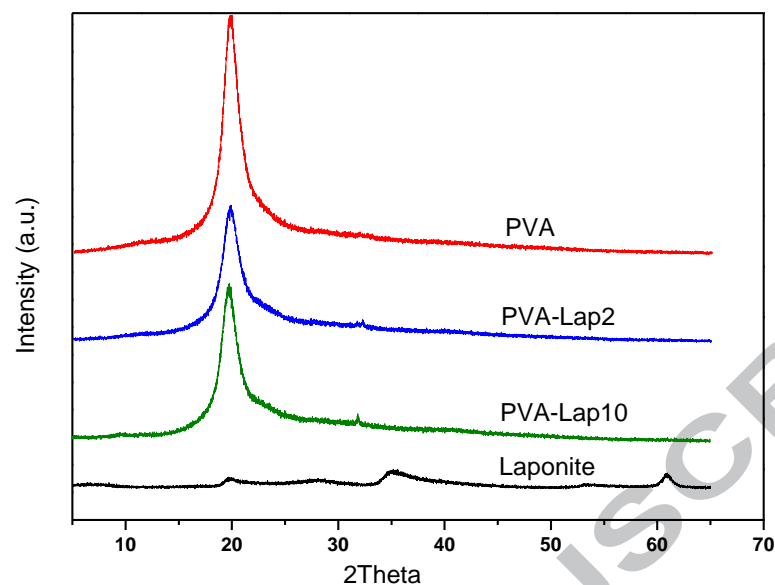


Figure 2 : XRD patterns of Laponite XLG powders, pristine PVA and PVA-Laponite mixed matrix membranes.

As observed in SEM image, the surface micrograph in Fig. 3b represents the smooth and dense PVA pristine membrane. The surface and cross-sectional SEM images of PVA-Lap2 and PVA-Lap10 are shown in Fig. 2(c, d) and (e, f) respectively. As can be seen, the SEM images of the MMMs surface Fig.3 (c, e) confirm that laponite was homogeneously dispersed within the PVA matrix without any cracks or voids around the clay. However, compared to the pristine PVA, the surface of PVA-Laponite membranes appear rough and denser. The cross section of the PVA-Lap2 Fig.3 (d) displays uniform and homogenous dispersion of the clay in the polymer matrix indicating perfect exfoliation process. Incorporation of more nanoplatelets, PVA-Lap10, resulted in some agglomerations on the surface in addition to increasing the surface roughness Fig. 3(e). Moreover, when the clay loading reached 10 wt%, the clay was inclined to assemble together forming a separated layer intercalated with the polymeric matrix, which might affect the mechanical properties and pervaporation performance of the membranes. These results are in consistent with the analysis of XRD patterns.

The FT-IR spectra of laponite XLG powder, pristine PVA, and PVA-Lap2 MMMs are depicted in Fig.4. The laponite spectrum showed a multicomponent wide band between 3700 and 3000 cm^{-1} , which was assigned to the stretching and bending of surface hydroxyl groups (Si-OH and Mg-OH) and at 1630 cm^{-1}

related to adsorbed water on laponite XLG. The stretching of Si O and Si–O–Si bonds appeared as a strong band at 957 cm^{-1} and the stretching of Mg–O is ascribed by a band at 640 cm^{-1} [33, 47].

FTIR spectra of the pristine PVA showed a broad peak between 3590 and 3070 cm^{-1} indicating -OH groups involved in the inter- and intramolecular hydrogen bonds. No peaks could be observed in the range from 3700-3600 cm^{-1} , which demonstrates that all -OH groups were bonded. [21-23]. The bands between 2940 and 2900 cm^{-1} are due to C-H stretching vibration alkyl groups of PVA chains. Due to low Glutaraldehyde concentration (0.3 v/v%), the two peaks attributed to CH corresponding to aldehyde at about 2850 and 2750 cm^{-1} were not observed. The characteristic Peaks at 1425 and 1321 cm^{-1} belong to the symmetric bending and the wagging of CH_2 , 1300-1100 cm^{-1} due to CH and C–O–C from acetal ring resulted during the crosslinking reaction were also observed, respectively [48, 49].

The vibration peaks attributed to C–O chain, the angular deformation outside the plan of O–H bond and C–C in the PVA chain were identified at 1085, 920, and 831 cm^{-1} , respectively. Compared to the pristine PVA membrane, PVA-Lap2 FTIR spectrum displayed same peaks in addition to narrow peak band at 620 cm^{-1} due to Mg–O stretching. Moreover, the Si–O–Si stretching frequency peak at 920 cm^{-1} exhibited slight shift change toward higher value when compared with laponite. This shift can be attributed to the interactions between PVA polymer and the clay through Si–OH groups.

Figure 5 shows the TGA curves of laponite XLG, pure PVA membrane, and PVA-Lap2 MMMs. All samples presented the first weight loss step which is attributed to the water release (dehydration process occurring up to about 150 °C), realized more clearly in DTG curves than in TGA curves [29]. Laponite XLG clay is thermal stable up to about 700 °C; the clay layers dihydroxylation process is observed above this temperature. Pure PVA membrane exhibited a second failure between 200 – 350 °C according to DTG curves, which was assigned to the decomposition of the side chain of PVA. Finally, the third thermal degradation which split into two stages between 350 – 450 °C and 450- 580 °C and this can be attributed to the decomposition of the backbone of PVA and the carbonated residue such as glutaraldehyde respectively [50, 51].

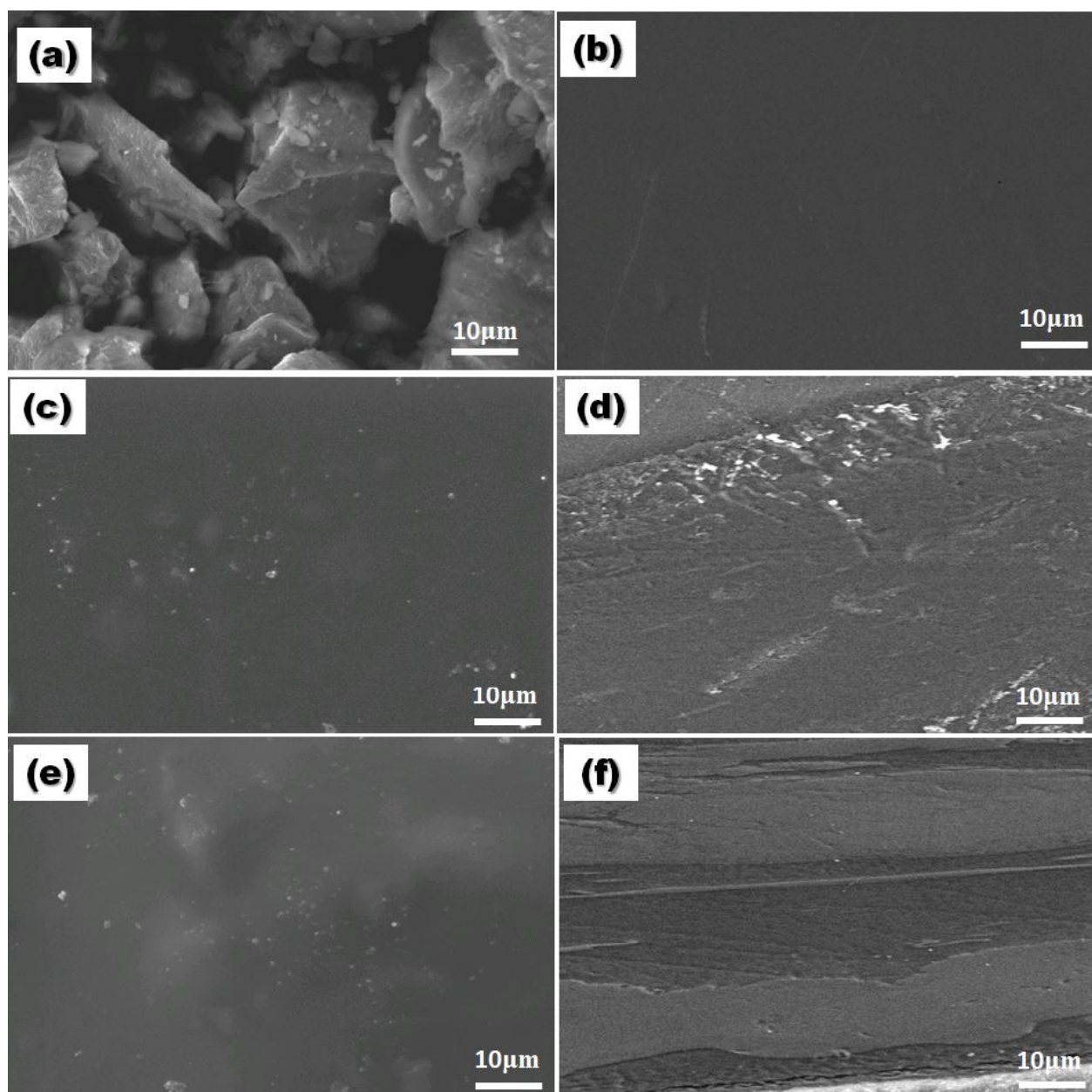


Figure 3: SEM images of laponite powder (a) pristine PVA (b) surface and cross-section of (c, d) PVA-Lap2, (e, f) PVA-Lap10 membranes.

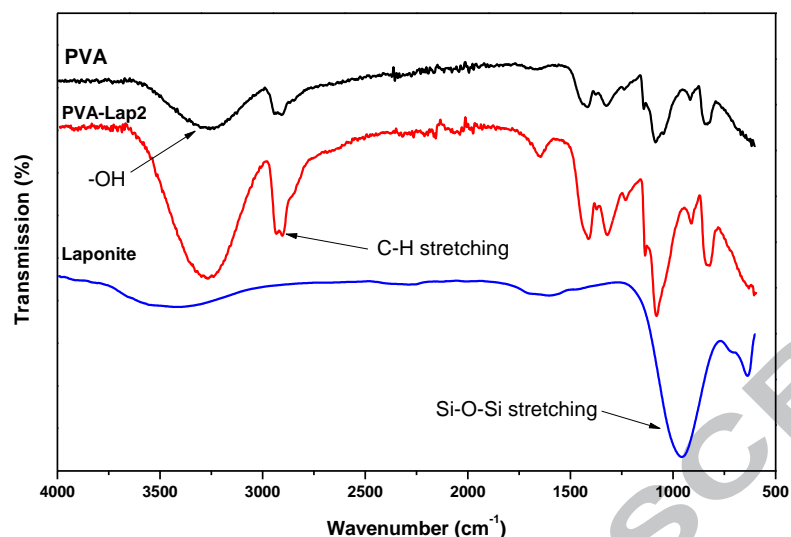


Figure 4: FTIR spectrum of Laponite XLG powder, pure PVA, and PVA-Lap2 membrane.

Although there was no significant change in weight loss of the plain and laponite XLG-loaded membrane, the thermal degradation temperature of mixed matrix membrane was much higher than that of the pure membrane due to the laponite addition into the PVA matrix. While the degradation temperature for 30% weight loss for PVA pure membrane was around 277 °C, that it was 377 °C for the 2 wt% laponite incorporated mixed matrix membrane.

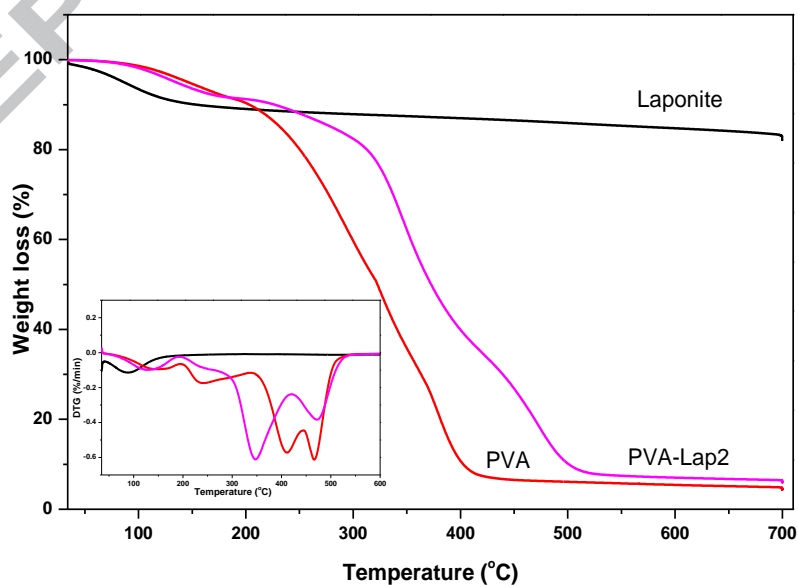


Figure 5: TGA and DTG curves of the laponite XLG powder, pure and PVA-Lap2 MMMs.

Hydrophilicity

Based on the solution diffusion model in pervaporation desalination, water adsorption on the surface of the membrane is the first step in the water transport which is attributed to the surface hydrophilicity of the membrane. The PVA and PVA-Lap MMMs surface hydrophilicity were elaborated by water contact angle measurement using a sessile drop methodology. As shown in Fig. 6 (a), increasing the laponite content led to decrease in water contact angle. It can be owing to the high hydrophilic surface of the laponite XLG [30]. Therefore, the contribution of laponite made the membranes rougher and more hydrophilic which may contribute to an enhancement of the water permeation through the membrane. Additionally, as can be observed, at high laponite content the increase in water contact angle of MMMs started to show stable values.

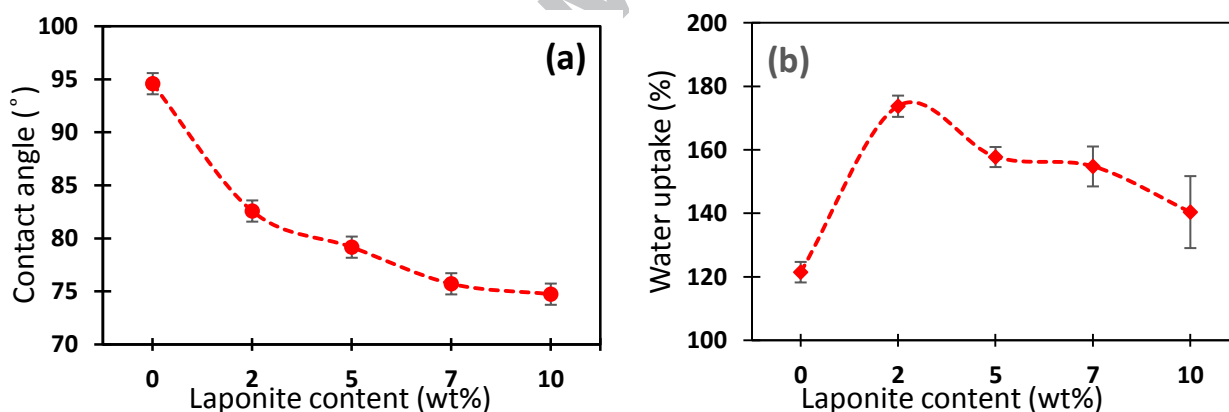


Figure 6 : (a) Water contact angle and (b) water uptake of PVA and PVA-Lap membranes.

The swelling behavior of membranes is generally delineated by the water uptake results. The influence of different laponite XLG content on the swelling behavior of the membranes was investigated in water at room temperature is displayed in Fig. 6 (b). It can be observed from the figure that the in the beginning the water uptake increases to a maximum value at 2 wt% laponite and then gradually decreases with higher laponite content in the membranes. The initial increase could be attributed to the higher hydrophilicity behavior of the membrane[32], while the decrease with higher laponite loading can be associated with the accretion of the physical crosslinking due to the presence of clay which could act as a

physical crosslinker in addition to the chemical crosslinker GA which decreases the free volume of PVA matrix and restricts the dissolution of polymer in water[52].

Mechanical properties

One of the main characteristic properties of a membrane is the mechanical stability and mechanical strength. It has been reported that incorporation of nanomaterials such as nanoclay in the polymer matrix is a powerful and easy way to improve the polymer stability [27]. To study the influence of laponite on the mechanical properties of PVA membrane, a tensile test was accomplished. Figure 7 presents the test results of yield stress and Young's modulus of the PVA-Lap. MMMs. For instance, yield stress and Young's modulus demonstrate similar inclination. Hence, it was found that addition of 2 wt% laponite enhanced the yield stress and Young' modulus by 35% and 62% respectively compared to the pure PVA membrane. These results could be attributed to the strong interconnection among the nanoclay and the polymer matrix and the fact is that laponite acts as a physical crosslinker. Similar results have been reported [52].

Nevertheless, a further increase in the laponite content led to a significant reduction in the mechanical properties of membranes. It was assigned that, at low content, laponite displays uniform and homogenous dispersion in the PVA matrix indicating perfect exfoliation process and had good adhesion with the polymer matrix. While increasing the laponite content, nanoplatelets tend to agglomerate leading to weak interaction between laponite and PVA resulting in tacky adhesion with polymer matrix and thus lower membrane mechanical properties. Du et al. [53] demonstrated similar phenomenon that the laponite-poly (acrylic acid) nanocomposite show maximum yield stress at 0.14 wt% laponite content and then decrease by increasing the clay loading. These results proved that 2 wt% laponite XLG nanoplatelets significantly improve the mechanical properties of PVA membrane.

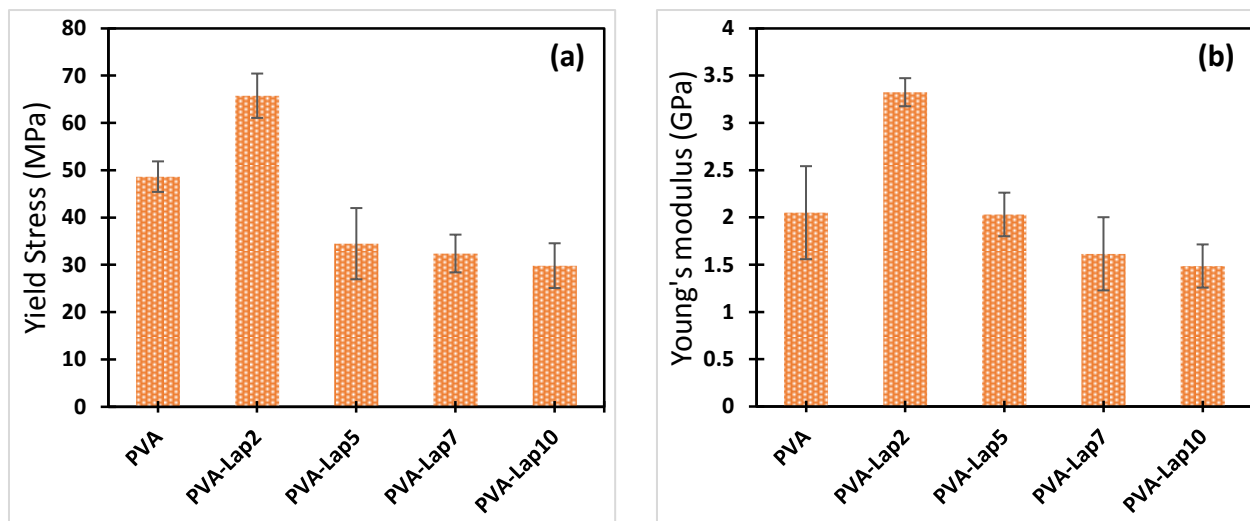


Figure 7: Effect of laponite XLG on the mechanical properties of the mixed matrix membranes; (a) yield stress and (b) Young's modulus of the MMMs as a function of laponite content.

3.2. Pervaporation experiment

3.2.1. Effect of laponite XLG content

Fig.8 represents the effect of incorporation of different laponite content on the pervaporation desalination performance of PVA membrane. Regardless, the feed solution the flux first increased then decreased. PVA-Lap2 obtained the maximum flux of all feed solution irrespective of pure water or NaCl solution. A similar trend of water flux has been obtained in water uptake measurements.

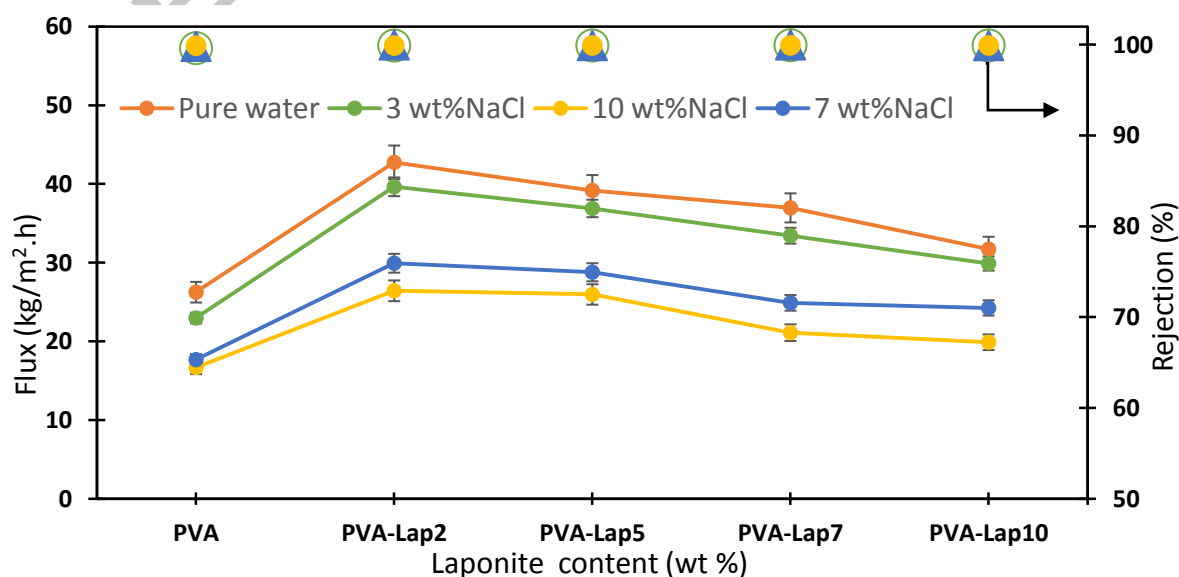


Figure 8: Pervaporation desalination performance of PVA-Lap MMMs at different laponite content at 40 °C.

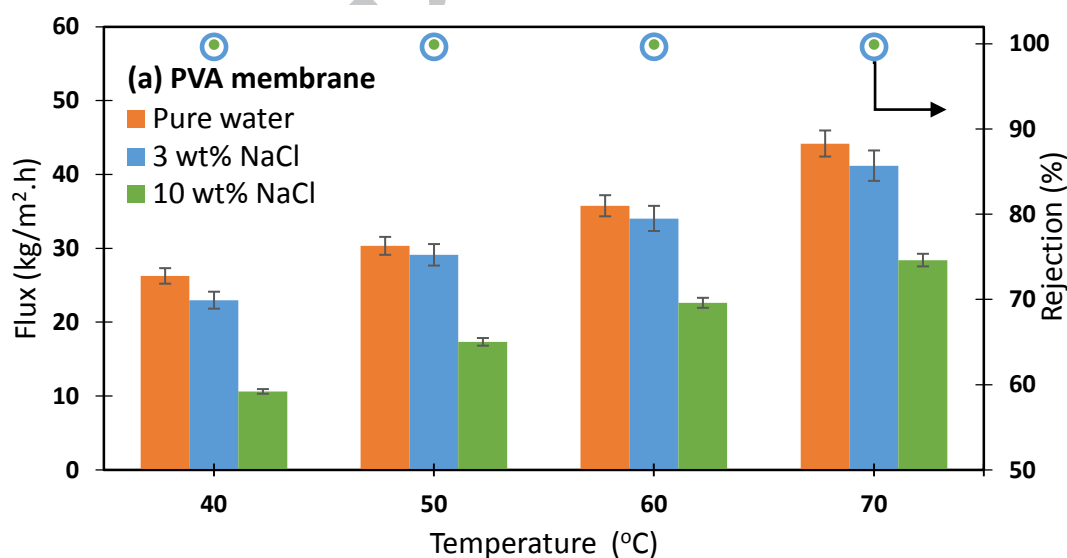
Based on the solution-diffusion mechanism, solubility and diffusivity of water in the membrane is controlling the water permeability in pervaporation desalination process[41]. The contribution of low content of laponite made the membranes rougher and more hydrophilic which may result in adsorption of more water to the membrane surface, thus making an enhancement in the water permeation flux through the membrane. However, by increasing the laponite content, nanoplatelets leading to restrict chain mobility of PVA which decrease water adsorption on active sorption sites of both the clay and PVA. In addition laponite could act as physical crosslinker leading to limit the affinity of PVA towards water, thus decreased the diffusion rate. Fig. 8 presents the salt rejection of the membranes preserved over 99.5% for the pristine PVA while increasing the amount of laponite led to increasing the salt rejection to over 99.9%.

This could be owing to the size exclusion mechanism during the pervaporative desalination process [54, 55]. Due to laponite exfoliation in the PVA matrix it would restrictive the free space of the polymer chain. Therefore, based on the size exclusion theory, water (0.27 nm) was easily penetrated compared to the hydrated ions (0.712 nm) and (0.664 nm) for Na⁺ and Cl⁻ respectively [56]. The augmentation in the rejection could be also imputed to the stated fact that the surface charge of membrane and the ions concentration in the feed can play an important role in desalination performance [37, 54, 57]. Based on the charge exclusion theory, the ions with the same charge as that of the surface of the membrane will get rejected and remain in the feed side. As Laponite nano-disc is reported as negatively charged surface and positively charged edge clay. Accordingly, for a water-NaCl solution, the negative surface of the clay will positively be charged with the sodium ions, and rejection is consisted on hydrated chlorine ions. Therefore, the ion separation in the PVA-Lap MMMs relies on the dispersion of clay in the PVA matrix and on the allocation of the Surface/edge of the laponite discs.

3.2.2. Effect of operating temperature

Despite the membrane properties and characteristic of permeant are the main parameters on a membrane representation on the PV separation, yet process operating conditions such as operating temperature could show high influence on the separation performance. The temperature is a dominant factor for the pervaporation separation process as changing the temperature can influence solubility and diffusivity of water within the membrane [58]. Additionally, the temperature has a significant effect on water vapor pressure on the feed side, while is almost obsolete due to the vacuum process in the cold traps. Therefore, rising the temperature results in a considerable increase in the driving force and thus the permeation of water across the membrane [59].

The effect of feed temperature on the desalination separation performance was investigated. Fig. 9a and b show the performance of PVA membrane and PVA-Lap2 MMMs at different feed temperatures and concentrations. For the pristine PVA membrane, all the salt rejections are above 99.5% for all the concentration and the water flux increases with increasing the temperature by around 70 % for the pure water and 3 wt% NaCl solution in the temperature range of 40–70 ° C.



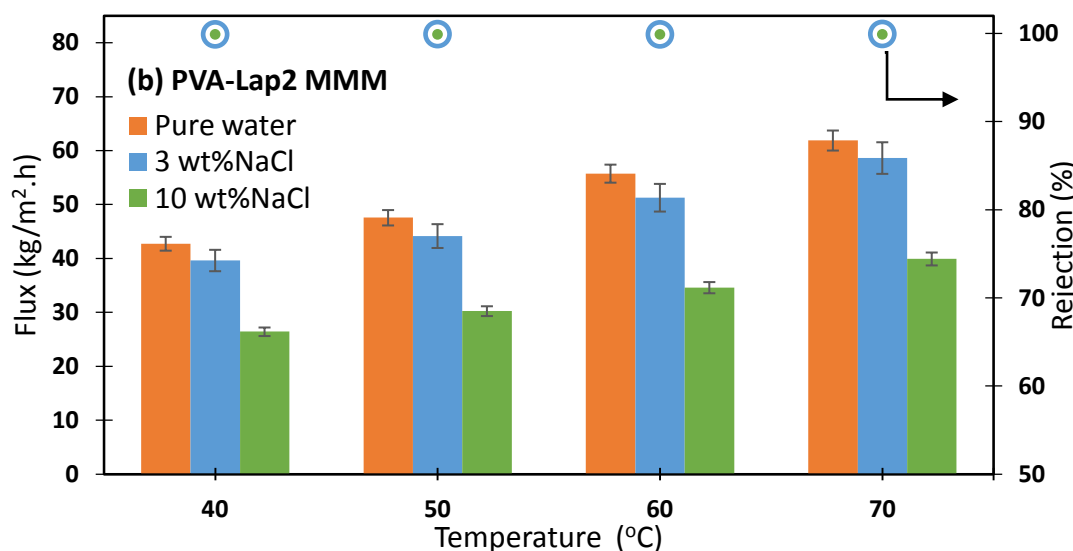


Figure 9: Pervaporation desalination performance at different salt concentration and temperature of (a) PVA membrane, and (b) PVA-Lap2 MMM.

On the other hand, for all the concentration, the PVA-Lap2 MMM shows a salt rejection of over 99.9% no matter the feed temperature and displayed relatively high water flux of 58.6 kg/m².h and 39.9 kg/m².h for desalinating 3 wt% and 10 wt% NaCl solution respectively at 70 °C. These desirable results describe the advantages of increasing the feed temperature on the desalination pervaporation of high-salinity water. Moreover, it can be observed that by increasing the feed temperature along with increasing the feed concentration the water flux crucially decreased. The reason is that at a higher temperature, the vapor pressure of water became more influenced by feed concentration. Therefore, increasing the feed concentration results in decreasing the water permeation flux [20].

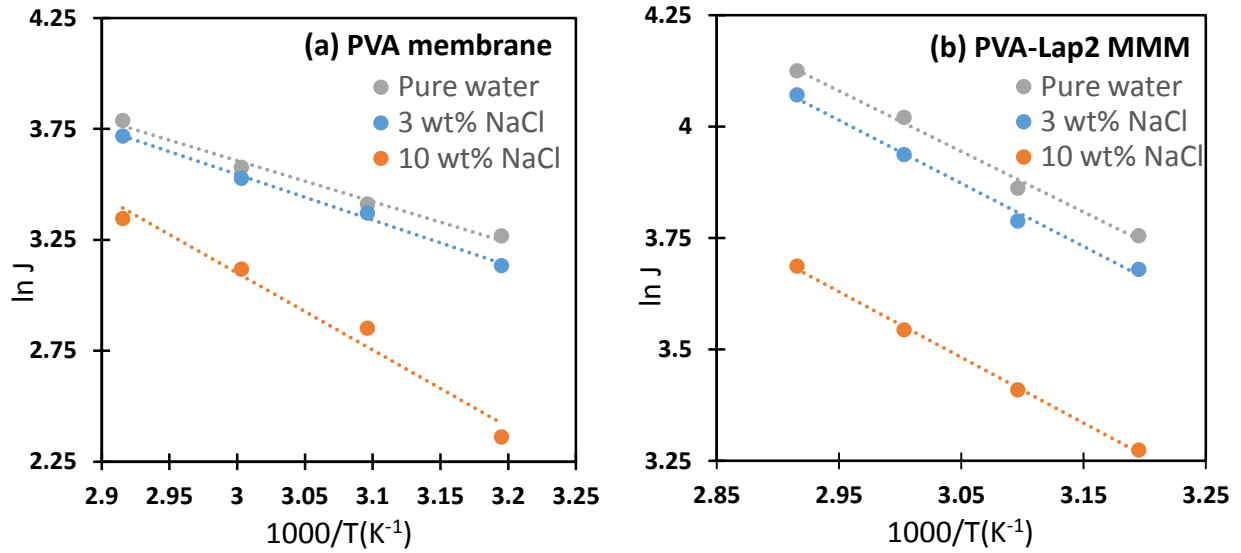


Figure 10: Arrhenius plot of flux vs temperature in desalination pervaporation at different feed concentration.

For further understanding of the influence of temperature on water permeability through the PVA-Lap membrane, the relationship between water flux and feed temperature follows the Arrhenius equation[60]:

$$J_i = A_i \exp\left(-\frac{E_{J,i}}{RT}\right) \quad (10)$$

where, the J_i is the component i flux of (kg /m².h), A_i is the pre-exponential factor (kg /m².h), $E_{J,i}$ is the apparent activation energy for component i transport through the membrane (kJ/mol), R is the gas constant (kJ/ mol.K) and T is temperature (K).

Fig. 10 a and b display the Arrhenius plot between water flux and feed temperature at different feed concentration. The results show a typical agreement with the model. The apparent activation energy for PVA membrane and PVA-Lap2 MMM at different feed concentrations was calculated from the slope of the Arrhenius plot E_J and the values are listed in Table 1. The values of E_J can be used as an assessment criterion of the required energy for i component to pass through the membrane material. For the component to diffuse easily through the membrane lower apparent activation energy is needed.

Table 1. : Activation energy for PVA and PVA-Lap2 membranes for pervaporation desalination of different NaCl

solutions.

Feed composition	Membrane	Activation energy (kJ/mol)
Pure water	PVA	15.36 ± 0.07
	PVA-Lap2	11.32 ± 0.04
3 wt% NaCl solution	PVA	17.05 ± 0.04
	PVA-Lap2	11.80 ± 0.04
10 wt% NaCl solution	PVA	28.87 ± 0.19
	PVA-Lap2	12.24 ± 0.02

From Table 1, one can observe that the activation energy required for PVA-Lap2 for all feed solution is significantly lower compared to PVA membrane. Moreover, increasing the feed concentration of PVA membrane led to a remarkable increase in the required energy. However, the desalination of 10 wt% NaCl solution using PVA-Lap2 results in the same low value of the activation energy. This indicates that incorporation of sufficient amount of laponite XLG clay has improved water permeability through the membrane and more suitable for water desalination.

Table 2: Comparison of desalination performance using other membranes reported in the literature for desalination of NaCl.

Membrane material	Temperature (°C)	NaCl concentration (wt %)	Flux (kg/m ² .h)	Rejection (%)	Reference
PVA/PS HF	70	3	7.4	99.9	[17]
PVA/Silica	60	3	10.4	99.9	[61]
CS/GO-1	60	3.5	17.7	99.99	[19]
GO/PAN	90	3.5	65.1	99.8	[59]

MXene/PAN	65	3.5	85.1	99.5	[60]
NaA Zeolite	69	3.5	1.9	99.9	[57]
PVA-Lap2	60	3	51.2	>99.9	This study
PVA-Lap2	70	3	58.6	>99.9	This study

Table 2 summarizes the pervaporation desalination performance of reported membranes in the literature. It can be seen that compared with other PVA membranes, PVA-Lap2 MMM showed a high rejection with excellent water flux at the same time. Additionally, compared to other polymeric membranes such as (CS/GO-1), composite membranes (MXene/PAN), and inorganic membranes (NaA zeolite), our PVA-Lap MMM offers a great potential for pervaporation desalination application.

3.3. Salt transport properties

The pervaporation permeability and selectivity are dominated by solubility and diffusivity of components through the membrane. Diffusion coefficient of NaCl shows the diffusive capacity of salt solution through the membrane and this can be obtained from the kinetic desorption experiments, D_s [34, 35]. Fig. 11 represents a typical desorption curve for NaCl. Similar to earlier studies [19, 36], D_s was calculated using Eq. 4 for the linear region of the desorption curve slope.

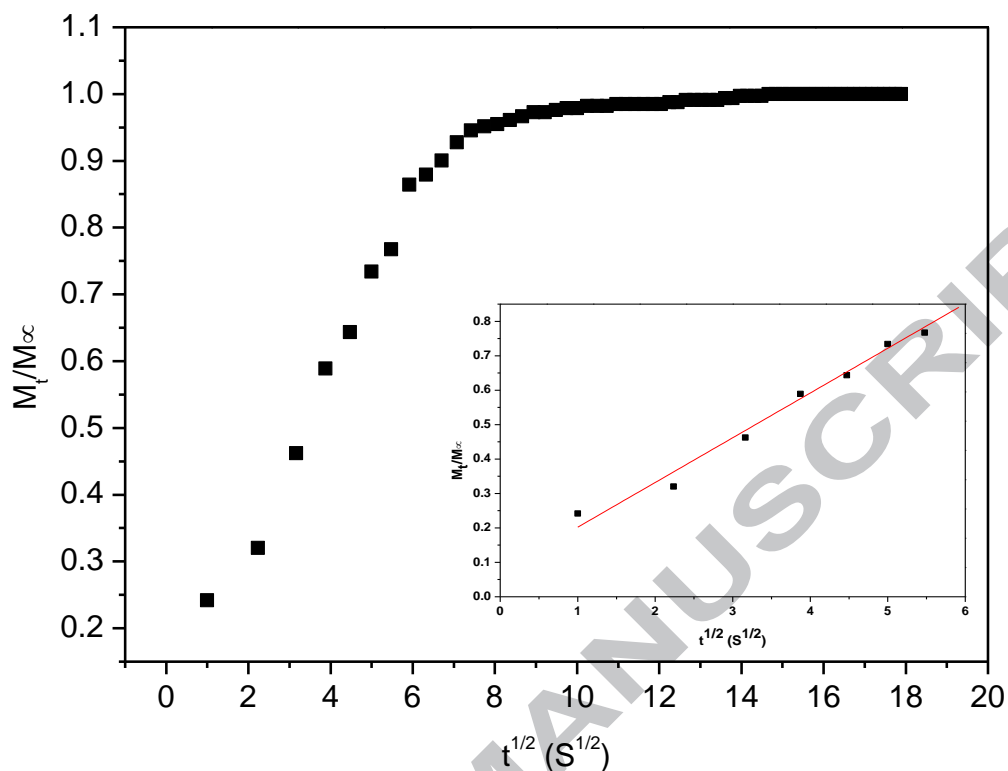


Figure 11: Typical NaCl desorption curve of PVA-Lap2 MMM for the measurement of NaCl diffusion coefficient.

Table 3 presents the salt diffusivity of MMMs as well as salt solubility and permeability calculated according to Eqs. 5 and 6 in section 2.4. Compared to PVA membrane, both salt diffusivity, D_s and solubility, K_s increased with increasing the laponite content up to 2 wt% then decreased with further increase in the clay content. Consequently, the salt permeability through the membrane is following the similar trend. These results are in consistent with the water uptake data. In theory, in a pure non-swollen polymer membrane no salt is expected to be dissolved, thus the adsorbed water in the membrane is supposed to dissolve any NaCl adsorbed in the membrane [40]. Therefore, the amount of water and NaCl in the membrane are closely correlated to each other.

Additionally, in order to calculate the membrane selectivity, the permeability of water was obtained from Eq. 9 and listed in Table 3. As can be seen, the water permeability coefficient exhibits similar tendency that is initially it gets increased followed by decrease with higher Laponite content. The results are attributed to the fact that with increase in the laponite content, the membrane hydrophilicity

increases while free volume of the membranes gets decreased. In addition to the physical crosslinking role of the nanoclay at higher loading which reduces the free volume and inhibits the water permeability increment with the enhancement in the membrane hydrophilicity. The maximum P_w that was achieved was approximately $11 \times 10^{-4} \text{ cm}^2/\text{s}$ at 2 wt% Laponite content. The value of permeability of water reached are remarkably high even compared to published data under comparable operating conditions [14, 36].

Table 3: Salt transport properties and water permeability through PVA and PVA-Lap MMMs with different clay content.

Membrane	D_s	K_s	P_s	P_w
	($\times 10^{-6} \text{ cm}^2/\text{s}$)		($\times 10^{-6} \text{ cm}^2/\text{s}$)	($\times 10^{-4} \text{ cm}^2/\text{s}$)
PVA	0.38	3.26	1.24	5.47
PVA-Lap2	0.64	3.72	2.36	10.69
PVA-Lap5	0.48	3.89	1.86	9.30
PVA-Lap7	0.47	3.66	1.72	8.78
PVA-Lap10	0.42	3.27	1.38	7.53

3.4. Permeation selectivity of membrane

When, water and salt permeability values in Table 3 are compared, it can be deduced that P_s is lower by two order of magnitude thereby indicating that water has preferential permeation through the membrane. The significant variation in permeability values of water and salt results in high water/salt selectivity as calculated using Eq. 8 and depicted in Fig. 12. This manifests that the amount of salt passing through the membranes is omitted compared to the amount of water. Fig. 12 displays that the increase in the laponite content in the membranes, the selectivity is increasing which is a counteractive trend to the water permeability through the membrane.

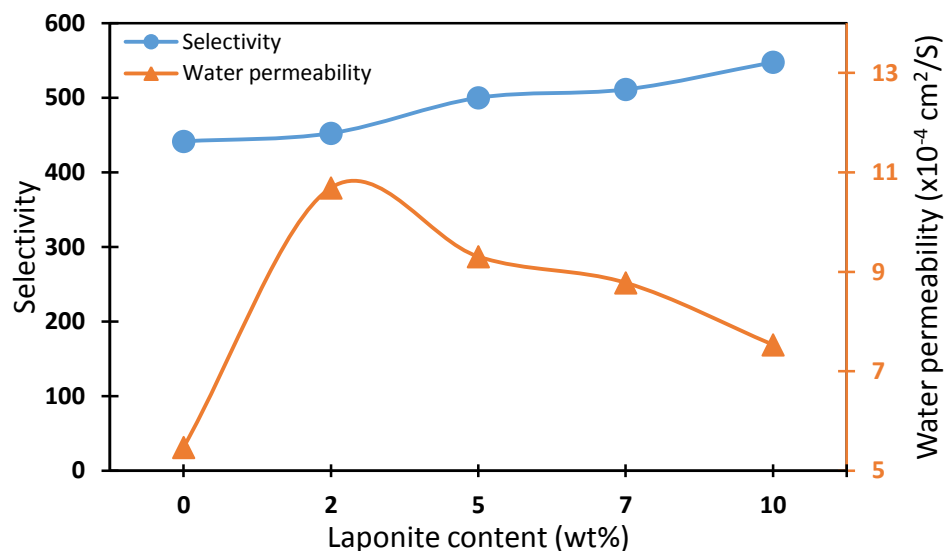


Figure 12: Water/salt selectivity and water permeability of PVA membrane and PVA-Lap MMMs with different laponite content.

This could be attributed to the solution-diffusion mechanism in which the free volume theory describes the transport in the dense membranes process as pervaporation. At higher content of laponite, more water is passing through the membranes according to the clay hydrophilic behaviour. However, the strong interaction between PVA matrix and clay as well as the physical crosslinking action of nanoplatelets result in decrease in the free volume of the mixed matrix membranes which cause decrease permeation in both water and salt while increasing selectivity. This result proves that high salt rejection in the pervaporation desalination process is a consequence of high water over salt permeability through the membrane.

4. Conclusion

Laponite XLG nanoclay was dispersed in water and exfoliated in PVA matrix to produce dense MMMs with several clay concentration for desalination by pervaporation. The MMMs surface hydrophilicity is increased with increasing the laponite content. The mechanical properties of the membrane were outstandingly enhanced by reaching 65.7 MPa and 3.3 GPa for the yield stress and young's modulus, respectively. In the beginning the MMMs water flux increased followed by decrease with a maximum value at 2 wt% laponite content. The salt rejection of the pristine PVA membranes preserved over 99.5%

while incorporation of the laponite clay led to improving the salt rejection to over 99.9%, this was attributed to the size/charge exclusion theory.

The permeability of water and salt permeability is according to the free volume theory when the laponite content increase in MMMs. In the pervaporation desalination process, it is not clear as to which factor affects salt rejection. Even the present study has shown that maximum water permeability across salt in dense membrane results in higher salt rejection in PV process. Two wt% laponite content PV membrane had fluxes of 58.6 kg/m².h and 39.9 Kg/m².h when desalinating 3 wt% and 10 wt% aqueous NaCl solution at 70 °C, respectively. However, the salt rejection still remained over 99.9% irrespective of the feed concentrations and temperatures. It can be concluded from this study that PVA-Lap MMMs is a promising and competitive candidate as far as pervaporation desalination is concerned.

Acknowledgements

The first author is grateful to Dr. Károly Renner, Polyak Peter and Bartos András for their help providing the clay and the thermal and mechanical properties measurements. This paper was supported by the János Bolyai Research Scholarship of the Hungarian Academy of Sciences, NTP-NFTÖ-18-B-0154, ÚNKP-18-4-BME-209 New National Excellence Program of the Ministry of Human Capacities, OTKA 112699 and 128543. This research was supported by the European Union and the Hungarian State, co-financed by the European Regional Development Fund in the framework of the GINOP-2.3.4-15-2016-00004 project, aimed to promote the cooperation between the higher education and the industry.

References

- [1] A. Subramani, J.G. Jacangelo, Emerging desalination technologies for water treatment: A critical review, *Water Res.*, 75 (2015) 164-187.
- [2] R.L. Mcginnis, M. Elimelech, Global Challenges in Energy and Water Supply: The Promise of Engineered Osmosis, *Environmental Science and Technology*, 42 (2008) 8625–8629.

- [3] H. Zhu, H. Wang, F. Wang, Y. Guo, H. Zhang, J. Chen, Preparation and properties of PTFE hollow fiber membranes for desalination through vacuum membrane distillation, *Journal of Membrane Science*, 446 (2013) 145-153.
- [4] Q. Wang, N. Li, B. Bolto, M. Hoang, Z. Xie, Desalination by pervaporation: A review, *Desalination*, 387 (2016) 46-60.
- [5] E. Drioli, A.I. Stankiewicz, F. Macedonio, Membrane engineering in process intensification—An overview, *Journal of Membrane Science*, 380 (2011) 1-8.
- [6] L.D. Tijging, Y.C. Woo, J.-S. Choi, S. Lee, S.-H. Kim, H.K. Shon, Fouling and its control in membrane distillation—A review, *Journal of Membrane Science*, 475 (2015) 215–244.
- [7] M. Drobek, C. Yacou, J. Motuzas, A. Julbe, L. Ding, J.C.D.d. Cost, Long term pervaporation desalination of tubular MFI zeolite membranes, *Journal of Membrane Science* 415–416 (2012) 816–823.
- [8] H.J. Zwijnenberg, G.H. Koops, M. Wessling, Solar driven membrane pervaporation for desalination processes, *Journal of Membrane Science*, 250 (2005) 235-246.
- [9] B. Liang, K. Pan, L. Li, E.P. Giannelis, B. Cao, High performance hydrophilic pervaporation composite membranes for water desalination, *Desalination*, 347 (2014) 199-206.
- [10] P. Shao, R.Y.M. Huang, Polymeric membrane pervaporation, *J. Membr. Sci.*, 287 (2007) 162-179.
- [11] A. Jonquière, R. Clément, P. Lochon, J. Néel, M. Dresch, B. Chrétien, Industrial state-of-the-art of pervaporation and vapour permeation in the western countries, *J. Membr. Sci.*, 206 (2002) 87-117.
- [12] N.G. Kanse, S.D. Dawande, A Review of Pervaporation Membrane System for The Separation of Ethanol/Water (Azeotropic Mixture), *International Journal of Engineering Sciences & Research Technology*, 4 (2015) 472-479.
- [13] A. Selim, N. Valentínyi, T. Nagy, A.J. Toth, D. Fozér, E. Haaz, P. Mizsey, Effect of silver-nanoparticles generated in poly (vinyl alcohol) membranes on ethanol dehydration via pervaporation, *Chin. J. Chem. Eng.*, (2018).

- [14] Z. Xie, M. Hoang, T. Duong, D. Ng, B. Dao, S. Gray, Sol-gel derived poly(vinyl alcohol)/maleic acid/silica hybrid membrane for desalination by pervaporation, *Journal of Membrane Science*, 383 (2011) 96–103.
- [15] M. Naim, M. Elewa, A. El-Shafei, A. Moneer, Desalination of simulated seawater by purge-air pervaporation using an innovative fabricated membrane, *Water Science & Technology* 72 (2015) 785–793.
- [16] D. Wu, A. Gao, H. Zhao, X. Feng, Pervaporative desalination of high-salinity water, *Chem. Eng. Res. Des.*, 136 (2018) 154–164.
- [17] S.G. Chaudhri, B.H. Rajai, P.S. Singh, Preparation of ultra-thin poly(vinyl alcohol) membranes supported on polysulfone hollow fiber and their application for production of pure water from seawater, *Desalination*, 367 (2015) 272–284.
- [18] R. Zhang, B. Liang, T. Qu, B. Cao, P. Li, High-performance sulfosuccinic acid cross-linked PVA composite pervaporation membrane for desalination, *Environ. Technol.*, 3 (2017) 1-9.
- [19] X. Qian, N. Li, Q. Wang, S. Ji, Chitosan/graphene oxide mixed matrix membrane with enhanced water permeability for high-salinity water desalination by pervaporation, *Desalination*, 438 (2018) 83-96.
- [20] L. Li, J. Hou, Y. Ye, J. Mansouri, Y. Zhang, V. Chen, Suppressing Salt Transport through Composite Pervaporation Membranes for Brine Desalination, *applied Sciences* 7(2017) 856-875.
- [21] J.M. Gohil, A. Bhattacharya, P. Ray, Studies on the Cross-linking of Poly(Vinyl Alcohol), *J.Poly.Res.*, 13 (2006) 161-169.
- [22] H. S.Mansur, C. M.Sadahira, A. N.Souza, A. A.P.Mansur, FTIR spectroscopy characterization of poly (vinyl alcohol) hydrogel with different hydrolysis degree and chemically crosslinked with glutaraldehyde *Mater. Sci. Eng., C*, 28 (2008) 539-548.
- [23] A. Hasimi, A. Stavropoulou, K.G. Papadokostaki, M. Sanopoulou, Transport of water in polyvinyl alcohol films: Effect of thermal treatment and chemical crosslinking, *Eur. Polym. J.*, 44 (2008) 4098–4107.
- [24] T. Jose, S.C. George, Induced Hydrophilicity of the Nanoclay on the Pervaporation Performance of Crosslinked Poly (Vinyl Alcohol) Nanocomposite Membranes, *Polymer-Plastics Technology and Engineering*, 55 (2016) 1266-1281.

- [25] S.G. Adoor, M. Sairam, L.S. Manjeshwar, K.V.S.N. Raju, T.M. Aminabhavi, Sodium montmorillonite clay loaded novel mixed matrix membranes of poly(vinyl alcohol) for pervaporation dehydration of aqueous mixtures of isopropanol and 1,4-dioxane, *Journal of Membrane Science* 285 (2006) 182-195.
- [26] S. Ravindra, V. Rajinikanth, A.F. Mulaba-Bafubiandi, V.S. Vallabhapurapu, Performance enhancement of the poly (vinyl alcohol) (PVA) by activated natural clay clinoptilolite for pervaporation separation of aqueous–organic mixtures, *Desalination and water treatment*, (2015) 1-15.
- [27] N. Golafshan, R. RezaHasani, M.T. Esfahani, M. Kharaziha, S.N. Khorasani, Nanohybrid hydrogels of laponite: PVA-Alginate as a potential wound healing material, *Carbohydr. Polym.*, 176 (2017) 392–401.
- [28] S. Wang, F. Zheng, Y. Huang, Y. Fang, M. Shen, M. Zhu, X. Shi, Encapsulation of amoxicillin within laponite-doped poly (lactic-co-glycolic acid) nanofibers: Preparation, characterization, and antibacterial activity., *ACS Applied Material Interfaces*, 4 (2012) 6393–6401.
- [29] G.F. Perotti, H.S. Barud, Y. Messaddeq, S.J.L. Ribeiro, V.R.L. Constantino, Bacterial cellulose-laponite clay nanocomposites, *Polymer*, 52 (2011) 157-163.
- [30] E. Wassel, M. Es-Souni, N. Berger, D. Schopf, M. Dietze, C.-H. Solterbeck, M. Es-Souni, Nanocomposite Films of Laponite/PEG-Grafted Polymers and Polymer Brushes with Nonfouling Properties, *Langmuir*, 33 (2017) 6739–6750.
- [31] L.M. Daniel, R.L. Frost, H.Y. Zhu, Edge-modification of laponite with dimethyl-octylmethoxysilane, *J. Colloid Interface Sci.*, 321 (2008) 302-309.
- [32] S. Morariu, M. Bercea, C.-E. Brunchi, Influence of Laponite RD on the properties of poly(vinyl alcohol) hydrogels, *J. Appl. Polym. Sci.*, (2018).
- [33] W. Liu, S. Yee, S. Adanur, Properties of electrospun PVA/nanoclay composites, *Journal of The Textile Institute*, (2013).
- [34] G.M. Geise, D.R. Paul, B.D. Freeman, Fundamental water and salt transport properties of polymeric materials, *Prog. Polym. Sci.*, 39 (2014) 1-42.

- [35] H. Ju, A.C. Sagle, B.D. Freeman, J.I. Mardel, A.J. Hill, Characterization of sodium chloride and water transport in crosslinked poly(ethylene oxide) hydrogels, *Journal of Membrane Science*, 358 (2010) 131-141.
- [36] Z. Xie, M. Hoang, D. Ng, C. Doherty, A. Hill, S. Gray, Effect of heat treatment on pervaporation separation of aqueous salt solution using hybrid PVA/MA/TEOS membrane, *Sep. Purif. Technol.*, 127 (2014) 10-17.
- [37] L. Ni, J. Meng, G.M. Geise, Y. Zhang, J. Zhou, Water and salt transport properties of zwitterionic polymers film, *Journal of Membrane Science*, 490 (2015) 73-81.
- [38] A.C. Sagle, H. Ju, B. D. Freeman, M.M. Sharma, PEG-based hydrogel membrane coatings, *Polymer*, 50 (2009) 756-766.
- [39] W. Xie, J. Cook, H.B. Park, B. D. Freeman, C.H. Lee, J.E. McGrath, Fundamental salt and water transport properties in directly copolymerized disulfonated poly(arylene ether sulfone) random copolymers, *Polymer*, 52 (2011) 2032-2043.
- [40] H. Yasuda, L.D. Ikenberry, R.L. Riley, Permeability of solutes through hydrated polymer membranes. I. Diffusion of sodium chloride, *Macromol. Chem. Phys.*, 118 (1968) 19-35.
- [41] Z. Xie, N. Li, Q. Wang, B. Bolto, Desalination by pervaporation, in: G. Gude (Ed.) *Emerging Technologies for Sustainable Desalination Handbook*, Elsevier Science, 2018, pp. 205-225.
- [42] J.G. Wijmans, R.W. Baker, The solution-diffusion model: a review, *Journal of Membrane Science*, 107 (1995).
- [43] S. Clémenson, D. Léonard, D. Sage, L. David, E. Espuche, Metal nanocomposite films prepared in situ from PVA and silver nitrate: Study of the nanostructuration process and morphology as a function of the in situ routes, *J. Polym. Sci., Part A: Polym. Chem.*, 46 (2008) 2062–2071.
- [44] M. Alexandre, P. Dubois, Polymer-layered silicate nanocomposites: preparation, properties and uses of a new class of materials, *Materials Science and Engineering*, 28 (2000) 1-63.
- [45] C.D. Delhom, L.A. White-Ghoorahoo, S.S. Pang, Development and characterization of cellulose/clay nanocomposites, *Composites: Part B*, 41 (2010) 475–481.

- [46] F.A. Aouada, L.H. Mattoso, E. Long, A simple procedure for the preparation of laponite and thermoplastic starch nanocomposites: Structural, mechanical, and thermal characterizations, *J. Thermoplast. Compos. Mater.*, 26 (2011) 109-124.
- [47] G.R. Mahdavinia, S. Mousanezhad, H. Hosseinzadeh, F. Darvishi, M. Sabzi, Magnetic hydrogel beads based on PVA/sodium alginate/laponite RD and studying their BSA adsorption., *Carbohydr. Polym.*, 147 (2016) 379–391.
- [48] B.Karthikeyan, Spectroscopic studies on Ag-polyvinyl alcohol nanocomposite films, *Physica B*, 364 (2005) 328–332.
- [49] M. Ghanipour, D. Dorrnian, Effect of Ag-Nanoparticles Doped in Polyvinyl Alcohol on the Structural and Optical Properties of PVA Films, *Journal of Nanomaterials*, 2013 (2013) 10.
- [50] H.G. Premakshi, A.M. Sajjan, A.A. Kittur, M.Y. Kariduraganavar, Enhancement of Pervaporation Performance of Composite Membranes Through In Situ Generation of Silver Nanoparticles in Poly(vinyl alcohol) Matrix, *J. Appl. Polym. Sci.*, 132 (2015) 1-11.
- [51] J.B. González-Campos, E. Prokhorov, I.C. Sanchez, J.G. Luna-Bárcenas, A. Manzano-Ramírez, J. González-Hernández, Y. López-Castro, R.E.d. Río, Molecular Dynamics Analysis of PVA-AgnP Composites by Dielectric Spectroscopy, *Journal of Nanomaterials*, 2012 (2012) 11.
- [52] S.H. Nair, K.C. Pawar, J.P. Jog, M.V. Badiger, Swelling and Mechanical Behavior of Modified Poly(vinyl alcohol)/Laponite Nanocomposite Membranes, *J. Appl. Polym. Sci.*, 103 (2007) 2896–2903.
- [53] J. Du, J. Zhu, R. Wu, S. Xu, Y. Tan, J. Wang, A facile approach to prepare strong poly(acrylic acid)/LAPONITE® ionic nanocomposite hydrogels at high clay concentrations, *RSC Advances*, 5 (2015) 60152–60160.
- [54] H. Yang, M. Elma, D.K. Wang, J. Motuzas, J.C.D.d. Costa, Interlayer-free hybrid carbonsilica membranes for processing brackish to brine salt solutions by pervaporation, *Journal of Membrane Science*, 523 (2017) 197–204.

- [55] W. An, X. Zhou, X. Liu, P.W. Chai, T. Kuznicki, S.M. Kuznicki, Natural zeolite clinoptilolite-phosphate composite Membranes for water desalination by pervaporation, *Journal of Membrane Science*, 470 (2014) 431–438.
- [56] F.U. Nigiz, N.D. Hilmioglu, Bentonite-loaded carboxy methylcellulose membrane for pervaporative desalination, *Desalination and water treatment*, 92 (2017) 20–26.
- [57] C.H. Cho, K.Y. Oh, S.K. Kim, J.G. Yeo, P. Sharma, Pervaporative seawater desalination using NaA zeolite membrane: Mechanisms of high water flux and high salt rejection, *Journal of Membrane Science*, 371 (2011) 226–238.
- [58] P. Schaetzel, C. Vauclair, Q.T. Nguyen, R. Bouzerar, A simplified solution – diffusion theory in pervaporation : the total solvent volume fraction model, *Journal of Membrane Science*, 244 (2004) 117-127.
- [59] B. Liang, W. Zhan, G. Qi, S. Lin, Q. Nan, Y. Liu, B. Cao, K. Pan, High performance graphene oxide/polyacrylonitrile composite pervaporation membranes for desalination applications, *J. Mater. Chem. A*, 3 (2015) 5140-5147
- [60] G. Liu, J. Shen, Q. Liu, G. Liu, J. Xiong, J. Yang, W. Jin, Ultrathin two-dimensional MXene membrane for pervaporation desalination, *Journal of Membrane Science*, 548 (2018) 548–558.
- [61] S.G. Chaudhri, J.C. Chaudhari, P.S. Singh, Fabrication of efficient pervaporation desalination membrane by reinforcement of poly(vinyl alcohol)–silica film on porous polysulfone hollow fiber, *J. Appl. Polym. Sci.*, 135 (2017).

- ✓ PVA/Laponite mixed matrix membranes were prepared using simple exfoliation process.
- ✓ MMMs were used for pervaporation desalination.
- ✓ High water permeability was achieved.
- ✓ Salt rejection of $> 99.9\%$ was maintained for all MMMs.
- ✓ Ability to desalinate high-salinity feeds.

ACCEPTED MANUSCRIPT